Conformational Cycle of a Single Working Enzyme

Noam Agmon*

The Fritz Haber Research Center, Department of Physical Chemistry, The Hebrew University, Jerusalem 91904, Israel

Received: April 4, 2000; In Final Form: May 30, 2000

By simultaneous analysis of the on-time distribution and autocorrelation function of a single working cholesterol oxidase enzyme, a diffusional model reveals the coupling of conformation change with enzyme action. Active-site oxidation induces a conformational change that opens the path for substrate entry. Its binding, in turn, induces the reverse protein relaxation process, which tightens the active site, thereby reducing the rate of product release.

1. Introduction

The idea that enzyme activity may depend on conformational change has been discussed extensively,[1−6] but a direct demonstration of the effect has not yet been produced. X-ray[7,8] and hydrogen−deuterium exchange data[9] suggest that enzymes assume different conformational states that change in response to substrate or cofactor binding. However, time-resolved data with a theoretical interpretation connecting, quantitatively, conformational change with enzyme activity are still to be obtained.

Such an understanding has been achieved for heme proteins, which transport and store oxygen. Laser photolysis measurements over very wide ranges of time and temperatures revealed inhomogeneous (distributed), near-power-law kinetics at low temperatures that slow at higher temperatures in some time range.[10] This effect was initially attributed to ligand escape[10] and subsequently to protein conformational relaxation.[11] In the latter scenario, the photodissociated heme protein finds itself in an unfavorable conformation and responds by slowly relaxing to a new equilibrium state, during which the rebinding rate dramatically diminishes. This gives rise to a "dynamic disorder" effect, as opposed to the "static disorder" observed at low temperatures or short times. "Kinetic hole-burning"[13,14] and multipulse experiments[15,16] were used to differentiate between these two heterogeneity components.

Such differentiation is straightforward in single molecule spectroscopy (SMS): the observation of a single molecule eliminates, by definition, the static disorder of the ensemble.[18] It has recently become possible to study single molecules at *room temperature*,[19] and this has paved the road for SMS studies of single biomolecules.[20] By monitoring the fluorescence from a pool of products,[21−24] single enzyme molecules were found to differ by over a factor of 10 in their activity, and this was attributed either to posttranslational modifications of their primary structure[23,24] or to differences in their conformation.[21,22]

In the time domain, single enzymes have been monitored by a variety of fluorescence techniques.[25−28] The present work focuses on the elegant experiments of Xie and co-workers[27,28] concerning the flavoenzyme cholesterol oxidase (COx) from soil bacteria. It catalyzes both the oxidation of cholesterol to its keto form and a double-bond isomerization.[29] Its active site, flavin−adenine dinucleotide (FAD), is naturally fluorescent, but after the oxidation of cholesterol, it becomes reduced ($FADH_2$), loosing its fluorescent properties. In a second step, $FADH_2$ is reoxidized by molecular oxygen. Crystal structure of the enzyme, refined at 1.8 Å resolution,[29] shows that the active site is buried within the protein. Thus, extensive conformational change should occur to allow a bulky cholesterol molecule to enter this site.

In the experiment,[27,28] single COx molecules were confined in agarose gel, with excess substrate and oxygen freely diffusing within the gel. The sample was illuminated with a cw laser through a microscope, and the fluorescence from the FAD active site was collected (with 13 ms time resolution). The emission showed on−off behavior as the enzyme cycled through its oxidized and reduced forms during catalytic activity. From these stochastic trajectories, the on-time distribution (OTD) and autocorrelation function (ACF) were computed for each individual enzyme. In a simple Michaelis−Menten (MM) scheme, in which an enzyme (E) binds a substrate (S), reacts, and releases its product (P), $E + S \rightleftharpoons ES \rightarrow E + P$, the kinetics are biexponential, with exponential rise and exponential decay. Such simplified kinetics cannot explain the long-time tail in the experimental data.

Consequently, models incorporating conformational change have been considered,[28] but only for the simplified two-state (ES and E + P) kinetics (applicable when the second step in the MM mechanism is rate-limiting). At least two types of models could account for the nonexponential ACF. These models are, however, incomplete. In the ligand coordinate, the binding step ($E + S \rightarrow ES$) should be introduced. In the protein coordinate, the reverse conformational change is missing. Clearly, during each enzyme cycle, any conformational change must be reset to enable the next activity cycle. A more complete model is presented below, which addresses these issues and demonstrates, for the first time, how both OTD and ACF are derived from the *same* model. In the emerging picture of this working enzyme, FAD oxidation induces a conformational change, which opens the way to the active site, whereas substrate binding induces the reverse relaxation process, which tightens the protein, thus *reducing* the rate of product release.

* Corresponding author: E-mail: agmon@fh.huji.ac.il. Fax: 972-2-6513742.

10.1021/jp0012911 CCC: $19.00
Published on Web 07/19/2000

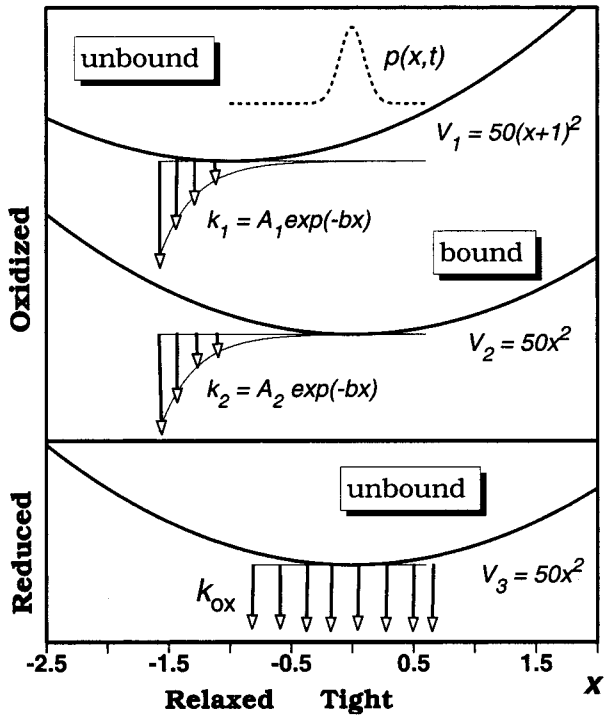

Figure 1. Detalied model for single COx action. For each of the three Michaelis−Menten levels, the conformational potentials, $V_i(x)$, are shown as bold curves, the sink terms $k_i(x)$ as arrows, and the initial distribution for an OTD calculation as a dashed curve. x is in arbitrary units. The parameters of the potential were not adjusted, but set arbitrarily to give $\Delta x = 1$ between the relaxed and tight states.

2. Model

The model depicted in Figure 1 consists of three MM states: E + S (MM1), ES (MM2), and E + P (MM3). As is customary, the EP state (bound product) is not explicitly represented. In MM1 and MM2, the FAD is oxidized and hence fluorescent, whereas in MM3, it is reduced to $FADH_2$ and hence nonfluorescent. The novelty of the picture is in the introduction of conformational substates, in a fashion that extends the irreversible case of heme proteins[11] (and related models for solvent-modulated electron-transfer reactions)[30,31] to reversible conformational changes in enzymes.

The suggested model involves a single, continuous conformational coordinate (x). In-line with the X-ray data[29] showing a buried active site, x may represent a protein mode gating the entry to this active site. The x motion is governed by a "potential", $V(x)$, better described as a free energy, arising from averaging over all other protein modes. It is measured here in units of thermal energy, k_BT. For a given MM state, there is a single minimum along this potential (at x_{min}), and not a double well representing a "two-level system" (TLS). This agrees with low-temperature hole-burning experiments on horseradish peroxidase,[32] which show that the hole widens as a power law in time (rather than logarithmically), in agreement with a diffusion model (rather than a TLS model). In this respect, the present picture differs from two-conformation models for this reaction.[28,33] However, the minimum along $V(x)$ may occur at different locations for *different* MM states, with x_{min} corresponding to either a "tight" (T) or "relaxed" (R) conformational state. R is characteristic of MM1, whereas T is characteristic of both MM2 and MM3. This allows the protein conformation to reset. When the unbound FAD is oxidized, the protein relaxes and pathways for substrate entry open. When the FAD is either bound or reduced, the protein tightens, making substrate entry or product escape difficult. The suggested initiation of these two relaxation processes is in accord with observations from other enzymes,[9] for which the binding of either substrate or small affectors induces conformational changes.

The transition from one MM level to another is governed by an *array* of rate constants. (Similarly, single lactate dehydrogenase molecules have different reactivities in their different equilibrium conformations.[21]) The transition from MM1 to MM2 and from MM2 to MM3 should be large for a relaxed protein, which allows binding of the substrate and unbinding of the product, diminishing rapidly as the protein becomes tighter. For simplicity, it is assumed that both obey the *same* exponential dependence, $k_i = A_i \exp(-bx)$, with only the pre-exponent (A_i) differing between MM1 and MM2. In line with the observations of Xie and co-workers,[27,28] the back reaction from MM2 to MM1 (substrate release) is neglected, and the transition from MM3 to MM1 is *not* distributed, so it is depicted by a single (x-independent) rate-constant, k_{ox}. This oxidation step depends on the diffusion of molecular oxygen into the active site. In contrast to bulky cholesterol, the small oxygen may find many paths into the protein without requiring large conformational changes, resulting in its rapid access into the protein core.[34]

The conformational probability density for each MM state, $p_i(x,t)$, can be obtained by solving three coupled diffusion (Smoluchowski) equations with the prescribed potential [$V_i(x)$] and sink terms [$k_i(x)$]

$$\frac{\partial p_i(x,t)}{\partial t} = D_i \frac{\partial}{\partial x} e^{-V_i(x)} \frac{\partial}{\partial x} e^{V_i(x)} p_i(x,t) + k_{i-1}(x)\, p_{i-1}(x,t) - k_i(x)\, p_i(x,t) \quad (1)$$

where $i = 1$, 2, or 3 and $k_0 \equiv k_3 = k_{ox}$. The diffusion constant on level i, D_i, determines the rate of conformational change on MMi. A set of *two* coupled equations of this type has been considered before, predominantly with the aim of estimating the effective rate constants.[35,36] Here, we focus on time-dependent properties, obtained numerically via a user-friendly PC package (SSDP ver. 2.6).[37] From the $p_i(x,t)$, evaluated for specified initial conditions, one can calculate the desired experimental attributes (see below).

Note how this differs from a prevalent approach that describes the time-dependence of conformational motion by an empirical stretched-exponential function.[12,26,38] Here, only the x dependence of potentials and sink terms is empirical; the time dependence follows from the solution of an equation of motion. This is not only a fundamentally more satisfying approach but also has practical advantages: when the potential can be determined from one type of experiment, the outcome of other experiments can be predicted without additional adjustable parameters.[39]

3. Attributes

The experimental observable (normalized fluorescence intensity ξ) is a two-valued function of the coordinate space, say $\xi = 1$ for the oxidized states (MM1 and MM2) and $\xi = 0$ for the reduced states (MM3). Denote these mutually exclusive parts of the conformational space by Ω_1 and Ω_0. Then, both the on-time distribution (OTD) and the autocorrelation function (ACF) can be calculated by evaluating appropriate transition probabilities between Ω_1 and Ω_0, which, in turn, can be obtained from the Green function of the equation of motion, eq 1. There is no need to simulate first a two-state trajectory analogous to the experimental one. Although this can be done, it will result in the unnecessary introduction of statistical noise.

3.1. On-Time Distribution. The "on time" is defined as the time between entry to Ω_1 and exit into Ω_0 (similarly, the "off time" is the time that elapses between entry into and exit from Ω_0). The OTD, $f_{on}(t)$, is the probability density for the on time to have duration t, namely, the flux out of Ω_1 given the (steady-state) flux into Ω_1 as the initial condition.[33] In the present model, the steady-state flux into the oxidized states is $k_{ox}p_3^{SS}(x)$. Because k_{ox} is not distributed, to a good approximation, the steady-state density in MM3, $p_3^{SS}(x)$, is proportional to $\exp[-V_3(x)]$. Thus, one sets $p_1(x,0) = p_3^{SS}(x)$ and $p_2(x,0) = p_3(x,0) = 0$, see dashed curve in Figure 1. The flux out of Ω_1 is, in the present case, the flux out of MM2, which is

$$f_{on}(t) \propto \int k_2(x)\, p_2(x,t|p_1 = p_3^{SS}, p_2 = p_3 = 0)\, dx \qquad (2)$$

where the initial condition ($t = 0$) appears to the right of the vertical line.

3.2. Autocorrelation Function. The importance of correlation functions for analyzing SMS data has been described.[38] The ACF can be evaluated most readily when the total observation time T is sufficiently long for the ergodic hypothesis to hold. It can then be written in two equivalent forms.[28] One involves averaging a single molecule property (say, f) over time, $\langle f\rangle = T^{-1}\int_0^T f(t')dt'$. The other involves averaging the Green function, $g(t,z|y)$, of the microscopic equation of motion over space ($\Omega_0 \cup \Omega_1$). Thus

$$C(t) \equiv \frac{\langle \Delta\xi(t')\, \Delta\xi(t+t')\rangle}{\langle [\Delta\xi(t')]^2\rangle} = \frac{\int\int dz\, dy\, [\Delta\xi(z)\, g(t,z|y)\, \Delta\xi(y)\, p^{SS}(y)}{\int dy\, [\Delta\xi(y)]^2\, p^{SS}(y)} \qquad (3)$$

describes the experimentally measured and theoretically computed ACF, respectively. $p^{SS}(y)$ is the steady-state solution for the equation of motion, and $\Delta\xi \equiv \xi - \langle\xi\rangle$.

Because $\xi(y)$ assumes two constant values, $\xi(\Omega_0) = 0$ and $\xi(\Omega_1) = 1$, the integrals in each region can be performed separately. Assuming that the observation time T is sufficiently long (otherwise, see refs 40 and 41) the time average of ξ approaches its steady-state limit $\langle\xi\rangle$. Under the same conditions, $\langle\Delta\xi^2\rangle = \langle\xi\rangle(1 - \langle\xi\rangle)$, and

$$C(t) = G_{00}(t|SS) + G_{11}(t|SS) - 1 \qquad (4)$$

where the effective Green function for transitions between domains Ω_0 and Ω_1 is given by

$$G_{ij}(t|SS) = \frac{\int_{\Omega_i} dz \int_{\Omega_j} dy\, g(t,z|y)\, p^{SS}(y)}{\int_{\Omega_j} dy\, p^{SS}(y)} \qquad (5)$$

($i, j = 0, 1$). Thus, the evaluation of $C(t)$ requires three propagations of the equation of motion. First is a long one to evaluate $p^{SS}(y)$, which is renormalized for each domain according to $p^{SS}(y|\Omega_i) = p^{SS}(y)/\int_{\Omega_i} dy\, p^{SS}(y)$ for $y \in \Omega_i$ and zero otherwise. Then, with $p^{SS}(y|\Omega_i)$ as the initial distribution, one evaluates the "survival probability" (spatial integral of the probability density) in domain Ω_i to obtain $G_{ii}(t|SS)$.

4. Results

Figure 2 shows a simultaneous fit of the model to the OTD and ACF of a single COx molecule reacting with a slow substrate.[27] Equation 1 was solved numerically using a readily available Windows package, SSDP ver. 2.6,[37] to obtain the probability densities, $p_i(x,t)$, on the various MM levels. Subsequently, $f_{on}(t)$ and $C(t)$ were calculated from eqs 2 and 4, respectively. Although it is possible to fit the OTD alone using a wide range of parameters, the requirement of a simultaneous agreement with the ACF data severely restricts the freedom in adjusting the parameters given in Table 1 (see also Figure 1). The parameter b should be sufficiently large to give strongly varying rate functions, $k_1(x)$ and $k_2(x)$, which produce the long-time tail. Although this tail exists in the OTD (see inset of Figure 2a), it is partly lost in the noise, whereas it is unmistakable in the ACF (see inset of Figure 2b).

For cholesterol itself, only the OTD was reported.[27] In Figure 3, it is fit by modifying b, A_1, A_2, and D_1 (whereas D_2, D_3, and

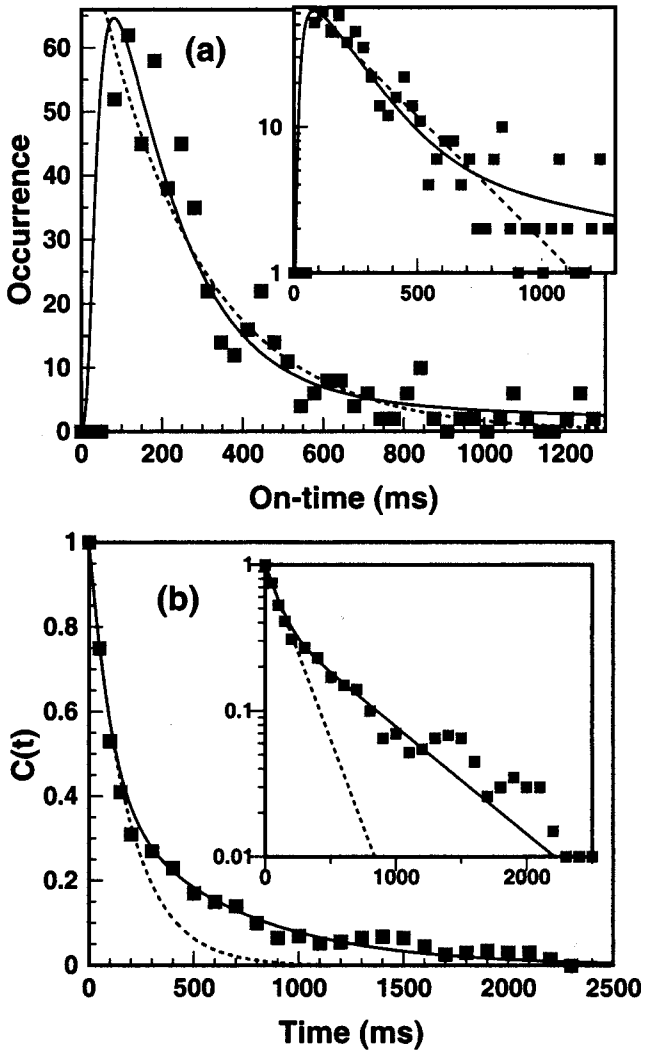

Figure 2. Simultaneous fit to (a) the OTD and (b) the ACF of a single COx molecule with 2 mM 5-pregene-3β-20α-diol substrate. Data (squares) from Figure 2 of ref 27. Solid line is the fit to the model depicted in Figure 1, obtained from a numerical solution[37] of eq 1 with the parameters of Table 1. Dashed line is the exponential decay from ref 27. Insets show the same data on a semilog scale.

TABLE 1: Model Parameters for COx Kinetics[a]

figure	b (Å^{-1})	A_1 (s^{-1})	A_2 (s^{-1})	D_1 (cm^2/s)	$D_2 = D_3$ (cm^2/s)	k_{ox} (s^{-1})
2	3.5	0.2	0.7	1×10^{-16}	8×10^{-18}	4
3a	3.0	0.3	1	1.5×10^{-17}	8×10^{-18}	NA
3b	3.0	4	0.8	1.3×10^{-16}	8×10^{-18}	NA

[a] Units of D_i correspond to x (Figure 1) in angstroms.

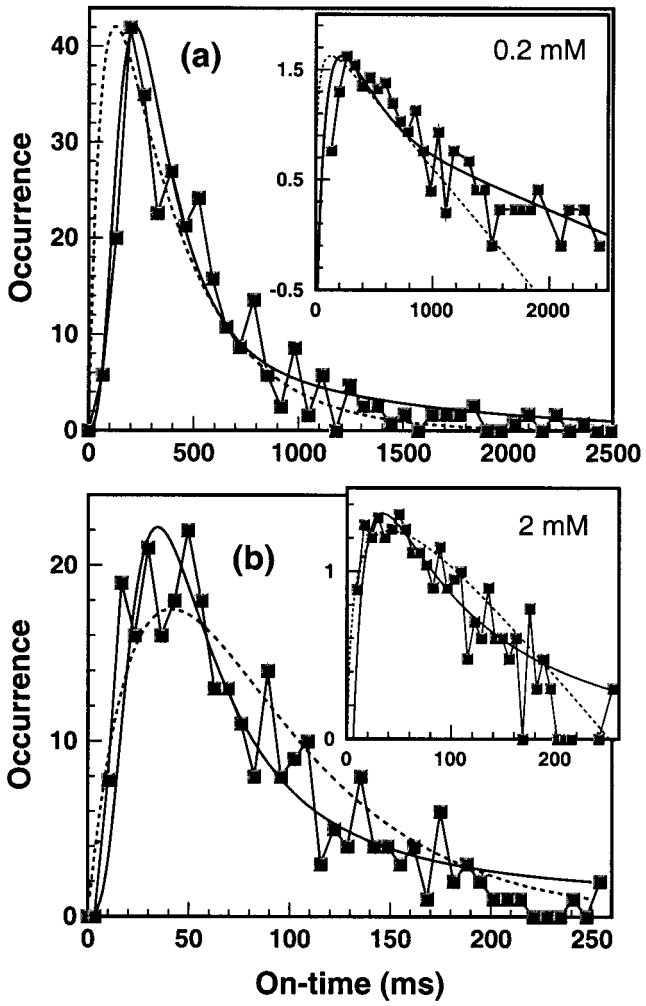

Figure 3. OTD for single COx molecule with (a) 0.2 mM and (b) 2 mM cholesterol substrate. Data (squares) from Figure 1c,d of ref 27. Solid line is the fit to the model depicted in Figure 1, obtained from a numerical solution[37] of eq 1 with the parameters of Table 1. Dashed line is the biexponential MM scheme from ref 27.

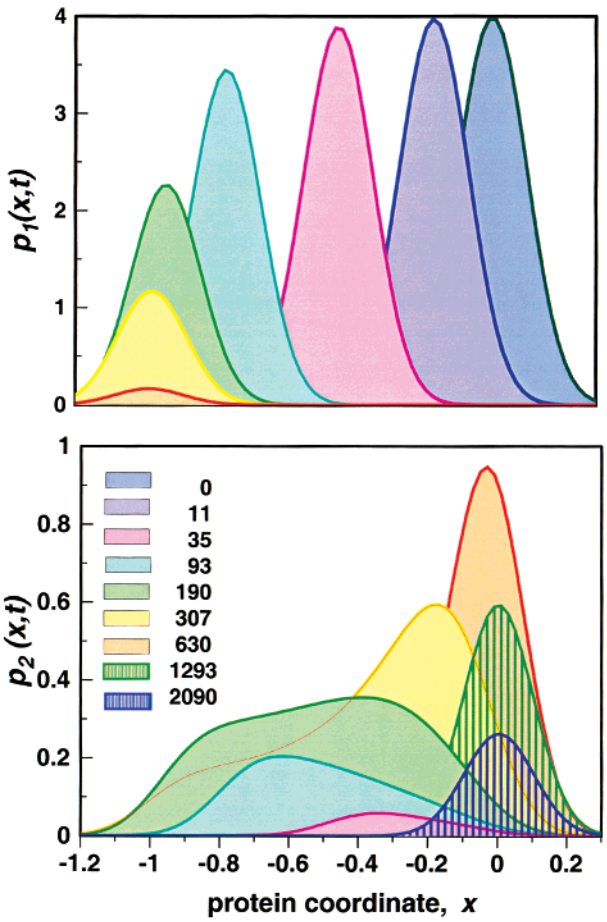

Figure 4. Conformational probability distribution for oxidized/unbound and bound single COx molecule with 0.2 mM cholesterol, from beginning to end of an on event (conditions of Figure 3a). Times (in milliseconds) are color-coded using the same key for both MM levels. Note how the chemical reaction on MM2 turns on (negative x), and then off again.

the parameters of the potential were not adjusted). The two data sets in panels a and b correspond to a factor of 10 in cholesterol concentration, which is manifested in nearly a factor of 10 in the binding rate coefficient, k_1 (see A_1 in Table 1). The model is capable of generating a delay in the OTD rising phase (Figure 3a), which is impossible to obtain using biexponential MM kinetics (dashed lines in Figure 3). However, D_1 changes by nearly a factor of 10 with concentration (Table 1), which might not be reasonable. A larger value of D_1 for $c = 0.2$ mM eliminates the delay in the rising phase in Figure 3a, and this could agree with more recent unpublished data.[42]

To understand how the nonexponentiality comes about, it is instructive to consider the time evolution of the conformational distribution for the oxidized/unbound and bound states (MM1 and MM2, respectively). Figure 4 shows such a (color-coded) time evolution, under the conditions of Figure 3a. The initial distribution is a normalized Gaussian, $p_3^{SS}(x)$, centered at the origin on MM1. Up to 30 ms, it relaxes to smaller x values without a loss in amplitude. As it approaches the region with larger $k_1(x)$, substrate binding begins, producing $p_2(x,t)$, whose peak initially traces that of $p_1(x,t)$. These events characterize the sigmoidal rising phase of the OTD (see Figure 3a). By the time of the OTD peak, $p_2(x,t)$ becomes very wide, covering a large part of conformation space (green profile). This leads to multiexponential decay. The initial fast decay is contributed from conformations centered at $x = -0.8$, which react very rapidly, possibly prior to any relaxation on MM2. In contrast, conformations centered near $x = -0.3$ relax on MM2 toward $x = 0$ (yellow and orange profiles). When this second relaxation phase is completed, they proceed to decay exponentially, without further change in shape (hashed profiles), giving rise to the slow tail of the OTD.

5. Conclusion

Enzymes are microscopic machines that couple conformational change to chemical activity. Developments in SMS, together with the theoretical model presented in this communication, produce the first detailed description of this effect. The COx enzyme studied by Lu et al.[27] exhibits two protein relaxation processes. In the first, triggered by FAD oxidation, the protein relaxes to allow substrate (cholesterol) entry. The second, triggered by substrate binding, tightens the protein, thus slowing product release. The first relaxation process could be manifested in a sigmoidal delay of the OTD rising phase, whereas the second produces the nonexponential decay that is particularly evident in the ACF.

It is amusing to consider whether, in addition to the geometrical role of the protein relaxation processes in allowing entry to and exit from the active site, it also has energetic implications. Indeed, this enzyme functions analogously to a microscopic heat (Carnot) engine. The first relaxation is a

thermal expansion process, during which heat is abstracted from the surrounding. The second protein relaxation is a thermal compression process, during which some heat returns to the surrounding and some is utilized to carry out a chemical reaction.

The analysis was performed using a diffusional model that extends a known model for heme proteins.[11] However, it is not at all clear that the relaxation process observed for COx is of a type similar to that detected in myoglobin. The latter terminates by about 1 μs at room temperature[16] and appears to be localized near the active site and decoupled from the surrounding solvent.[17] In COx, the relaxation processes occur on the time scale of 10−1000 ms and extends to the surface of the protein, where ligand entry is gated. Given the hierarchical nature of protein relaxation processes,[43] it is not inconceivable that faster protein relaxation processes take place in COx as well. These, at present, are outside the time resolution of SMS experiments.

Because the model is based on only the limited amount of data currently available, its details could change with future experimentation. For example, it was assumed that transition to the relaxed (R) protein conformation occurs only after FAD oxidation. If this is indeed the case, then the slowing of protein relaxation in MM1 should lead to enhanced delay in the OTD rise time. If, however, the R conformation is attained already in MM3, such a delay might not be expected. It could be interesting to check this point by repeating the measurements at lower temperatures.

The accuracy of the reported experimental data is insufficient for distinguishing between diffusion models and other simplified descriptions.[28] It is therefore desirable to obtain independent experimental evidence for protein relaxation, for example, by placing an acceptor and donor in strategically selected positions along the protein backbone.[25] Such positions are suggested by the X-ray studies,[29] which identified side loops that probably move to allow substrate entry. Their motion should correlate with the "on" and "off" events, as suggested from the present study.

A simple prescription allows one to calculate the ACF, irrespective of the complexity of the kinetic scheme. It involves the effective on−on and off−off transition probabilities, $G_{11}(t)$ and $G_{00}(t)$ of eq 5. Their sum is restricted at $t = 0$ and ∞ to equal 2 and 1, respectively, but otherwise they are independent. It might, therefore, be beneficial to calculate each one separately from the single-molecule trajectory, as was done in a recent single-channel study.[44] The simultaneous analysis of both the ACF and the OTD was seen to provide a powerful tool in distinguishing between molecular mechanisms. The ACF, which has been used extensively in noise analysis from excitable membranes,[45] has rarely been applied for single channels and then only in the simplest, exponential case.[46] Autocorrelation of dwell times has been more prevalent, but this measure was shown to be less sensitive to dynamic correlations.[28] Thus, the study of protein relaxation in single-channel experiments might also benefit from a simultaneous analysis of dwell times and current ACF.

It is important to note that there is presently no alternative to diffusive models of the type presented here. Conventional chemical kinetics are clearly oversimplified, whereas full-scale molecular dynamics is too demanding computationally and is presently incapable of describing events on time scales slower than a few nanseconds. The present model is of the right level of complexity, thus easily accessible computationally while producing meaningful physical insight.

Acknowledgment. I am indebted to X. Sunney Xie for advice concerning the data and comments on the manuscript and to U. Banin, A. M. Berezhkovskii, J. Cao, J. Jortner, S. Mukamel, and S. Weiss for discussions. The work was supported in part by the US-Israel Binational Science Foundation, Jerusalem, Israel. The Fritz Haber Research Center is supported by the Minerva Gesellschaft für die Forschung, mbH, München, FRG.

References and Notes

(1) Koshland, D. E., Jr.; Neet, K. E. *Annu. Rev. Biochem.* **1968**, *37*, 359−410.
(2) Agmon, N. *J. Theor. Biol.* **1985**, *113*, 711−717.
(3) Herschlag, D. *Bioorg. Chem.* **1988**, *16*, 62−96.
(4) Britt, B. M. *J. Theor. Biol.* **1993**, *164*, 181−190.
(5) Post, C. B.; Ray, W. J., Jr. *Biochemistry* **1995**, *34*, 15881−15885.
(6) Schienbein, M.; Gruler, H. *Phys. Rev. E* **1997**, *56*, 7116−7127.
(7) Perona, J. J.; Martin, A. M. *J. Mol. Biol.* **1997**, *273*, 207−225.
(8) Mundorff, E. C.; Hanson, M. A.; Varvak, A.; Ulrich, H.; Schultz, P. G.; Stevens, R. C. *Biochemistry* **2000**, *39*, 627−632.
(9) Halgand, F.; Dumas, R.; Biou, V.; Andrieu, J.-P.; Thomazeau, K.; Gagnon, J.; Douce, R.; Forest, E. *Biochemistry* **1999**, *38*, 6025−6034.
(10) Austin, R. H.; Beeson, K. W.; Eisenstein, L.; Frauenfelder, H.; Gunsalus, I. C. *Biochemistry* **1975**, *14*, 5355−5373.
(11) Agmon, N.; Hopfield, J. J. *J. Chem. Phys.* **1983**, *79*, 2042−2053.
(12) Steinbach, P. J.; Ansari, A.; Berendzen, J.; Braunstein, D.; Chu, K.; Cowen, B. R.; Ehrenstein, D.; Frauenfelder, H.; Johnson, J. B.; Lamb, D. C.; Luck, S.; Mourant, J. R.; Nienhaus, G. U.; Ormos, P.; Philipp, R.; Xie, A.; Young, R. D. *Biochemistry* **1991**, *30*, 3988−4001.
(13) Campbell, B. F.; Chance, M. R.; Friedman, J. M. *Science* **1987**, *238*, 373−376.
(14) Agmon, N. *Biochemistry* **1988**, *27*, 3507−3511.
(15) Post, F.; Doster, W.; Karvounis, G.; Settles, M. *Biophys. J.* **1993**, *64*, 1833−1842.
(16) Agmon, N.; Doster, W.; Post, F. *Biophys. J.* **1994**, *66*, 1612−1622.
(17) Agmon, N.; Sastry, G. M. *Chem. Phys.* **1996**, *212*, 207−219.
(18) Tamarat, P.; Maali, A.; Lounis, B.; Orrit, M. *J. Phys. Chem. A* **1999**, *104*, 1−16.
(19) Xie, X. S.; Trautman, J. K. *Annu. Rev. Phys. Chem.* **1998**, *49*, 441−480.
(20) Weiss, S. *Science* **1999**, *283*, 1676−1683.
(21) Xue, Q.; Yeung, E. S. *Nature* **1995**, *373*, 681−683.
(22) Tan, W.; Yeung, E. S. *Anal. Chem.* **1997**, *69*, 4242−4248.
(23) Craig, D. B.; Arriaga, E. A.; Wong, J. C. Y.; Lu, H.; Dovichi, N. J. *J. Am. Chem. Soc.* **1996**, *118*, 5245−5253.
(24) Craig, D. B.; Dovichi, N. J. *Can. J. Chem.* **1998**, *76*, 623−626.
(25) Ha, T.; Ting, A. Y.; Liang, J.; Caldwell, W. B.; Deniz, A. A.; Chemla, D. S.; Schultz, P. G.; Weiss, S. *Proc. Natl. Acad. Sci., USA* **1999**, *96*, 893−898.
(26) Edman, L.; Földes-Papp, Z.; Wennmalm, S.; Rigler, R. *Chem. Phys.* **1999**, *247*, 11−22.
(27) Lu, H. P.; Xun, L.; Xie, X. S. *Science* **1998**, *282*, 1877−1882.
(28) Schenter, G. K.; Lu, H. P.; Xie, X. S. *J. Phys. Chem. A* **1999**, *103*, 10477−10488.
(29) Vrielink, A.; Lloyd, L. F.; Blow, D. M. *J. Mol. Biol.* **1991**, *219*, 533−554.
(30) Zusman, L. D. *Chem. Phys.* **1983**, *80*, 29−43.
(31) Sumi, H.; Marcus, R. A. *J. Chem. Phys.* **1986**, *84*, 4894−4914.
(32) Schlichter, J.; Friedrich, J.; Herenyi, L.; Fidy, J. *J. Chem. Phys.* **2000**, *112*, 3045−3050.
(33) Cao, J. **2000**, *Chem. Phys. Lett.*, in press.
(34) Feher, V. A.; Baldwin, E. P.; Dahlquist, F. W. *Nat. Struct. Biol.* **1996**, *3*, 516−521.
(35) Berezhkovskii, A. M.; Zitserman, V. Y. *Chem. Phys.* **1991**, *157*, 141−155.
(36) Kurzyński, M. *Biophys. Chem.* **1997**, *65*, 1−28.
(37) Krissinel', E. B.; Agmon, N. J. *Comput. Chem.* **1996**, *17*, 1085−1098.
(38) Wang, J.; Wolynes, P. *Phys. Rev. Lett.* **1995**, *74*, 4317−4320.
(39) Agmon, N.; Krissinel', E. B. *Chem. Phys. Lett.* **1998**, *294*, 79−86.
(40) Geva, E.; Skinner, J. L. *Chem. Phys. Lett.* **1998**, *288*, 225−229.
(41) Berezhkovskii, A. M.; Szabo, A.; Weiss, G. H. *J. Chem. Phys.* **1999**, *110*, 9145−9150.
(42) Xie, X. S. Harvard University Department of Chemistry, 12 Oxford St., Cambridge, MA 02138. Personal communication.
(43) Frauenfelder, H.; Sligar, S. G.; Wolynes, P. G. *Science* **1991**, *254*, 1598−1603.
(44) Fuliński, A.; Grzywna, Z.; Mellor, I.; Siwy, Z.; Usherwood, P. N. R. *Phys. Rev. E* **1998**, *58*, 919−924.
(45) Neher, E.; Stevens, C. F. *Annu. Rev. Biophys. Bioeng.* **1977**, *6*, 245−381.
(46) Liebovitch, L. S.; Fischbarg, J. *Biochim. Biophys. Acta* **1985**, *813*, 132−136.